Molecular Dynamic Simulations of Ionic Liquid's Structural Variations from Three to One Layers inside a Series of Slit and Cylindrical Nanopores.

Ke Ma,[1, a)] Xuewei Wang,[2, 3] Jan Forsman,[4] and Clifford E. Woodward[5, b)]

[1)] *School of Materials Science and Engineering*
Tianjin University of Technology
Tianjin 300384, P. R. China

[2)] *School of Materials Science and Engineering, Tianjin University of Technology, Tianjin 300384, China*

[3)] *Tianjin Key Laboratory for Photoelectric Materials and Devices, Tianjin University of Technology, Tianjin 300384, China*

[4)] *Theoretical Chemistry, Chemical Centre, Lund University*
P.O.Box 124, S-221 00 Lund, Sweden

[5)] *School of Physical, Environmental and Mathematical Sciences*
University of New South Wales, Canberra at the Australian Defence Force Academy
Canberra ACT 2600, Australia

[a)]Electronic mail: kema@tjut.edu.cn

[b)]Electronic mail: c.woodward@adfa.edu.au

I. DONNAN POTENTIAL EXPRESSIONS

To estimate Donnan potential, incompressibility assumption is made. That is, the total solution of both neat IL and IL+solvent mixture are relatively incompressible.

$$n_i(z) = n_b exp(-\beta\mu_{ex}(z))exp(-\beta z_i(\psi(z) + \psi_{Donnan})) \tag{1}$$

in which n_b is the ion density in bulk, while z_i is the charge of ion type i. Set $i = +$ for cation and $i = -$ for anion Specifically, $z_+ = 1.0e$ for cation, and $z_- = -1.0e$ for anion. $\psi(z)$ is the electrostatic potential averaged over the plane at position z inside the pore. $\mu_{ex}(z)$ is the difference between the excess chemical potential in the pore and the bulk. The excess chemical potential term $\mu_{ex}(z)$ accounts for the non-electrostatic interactions, which are approximately the same for anions and cations as they have similar molar volume.

The number densities of cation and anion are then expressed as

$$\begin{aligned} n_+(z)exp(\beta e\psi(z)) &= n_b exp(-\beta(\mu_{ex}(z) + e\psi_{Donnan})) \\ n_-(z)exp(-\beta e\psi(z)) &= n_b exp(-\beta(\mu_{ex}(z) - e\psi_{Donnan})) \end{aligned} \tag{2}$$

By averaging $n_+(z)exp(\beta e\psi(z))$ and $n_-(z)exp(-\beta e\psi(z))$ in Eq.(2) over the pore volume, and taking the ratio of the two terms, we arrive at an approximation of the Donnan potential given by Eq.(3),

$$\begin{aligned} exp(-2\beta e\psi_{Donnan}) &= \frac{< n_+(z)exp(\beta e\psi(z)) >}{< n_-(z)exp(-\beta e\psi(z)) >} \\ &= \frac{\frac{1}{L}\int_0^L n_+(z)exp(\psi\beta e(z))\,dz}{\frac{1}{L}\int_0^L n_-(z)exp(-\psi\beta e(z))\,dz} \end{aligned} \tag{3}$$

in which e is the elementary charge, and $\beta = \frac{1}{kT}$ where k is Boltzmann constant, and T is temperature. Donnan potential expressions in the main text is thus obtained from Eq.(3) for all kinds of solutions studied in either slit or cylindrical pores.

II. CHARGE AND POTENTIAL PROFILES

A. Comparison between Slit and Cylindrical Pore

With regards to the capacitance comparison between slit and cylindrical pores, Figure 1 presents charge and potential comparisons at two distinct pore sizes: the slit capacitance

minimum at $L = 1.08nm$ and the slit capacitance maximum at $L = 1.63nm$. Electrostatic potential $\psi(z)$ at pore surface is set to zero as a reference level.

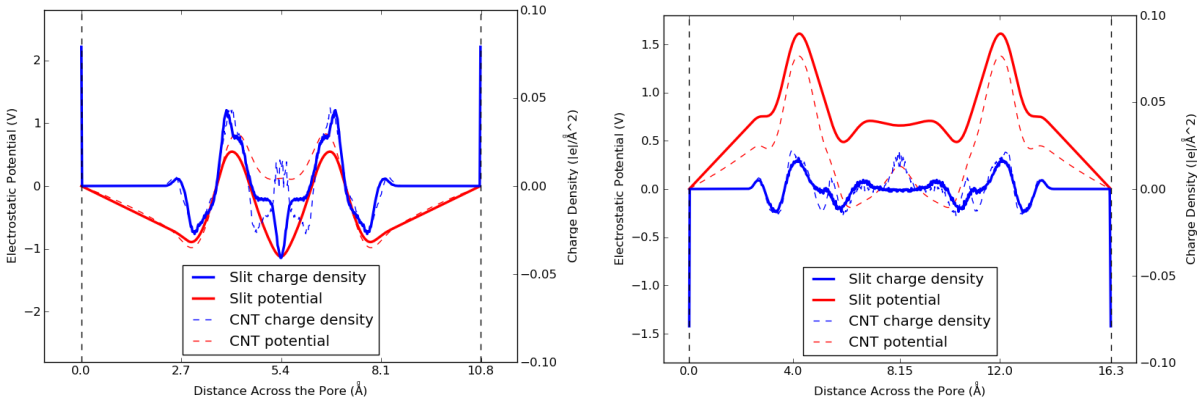

FIG. 1. Charge density and electrostatic potential profiles comparison between slit and cylindrical pore. On the left is positive electrode at pore size $L = 1.08nm$. On the right is negative electrode at pore size $L = 1.63nm$. $\psi(0)$ is set to zero. Dashed vertical lines represent the position of nanopore confinement.

B. Comparison of charge density distributions

The charge density distributions of $L = 2.03nm$ slit pore is plotted for pure IL inside both negative and positive pores, as illustrated in Figure 2. The charge densities oscillate to a smaller extent in the middle of the pore. The variation in charge density between negative and positive pores are more pronounced in the compact layer of the traditional electric double layer model.

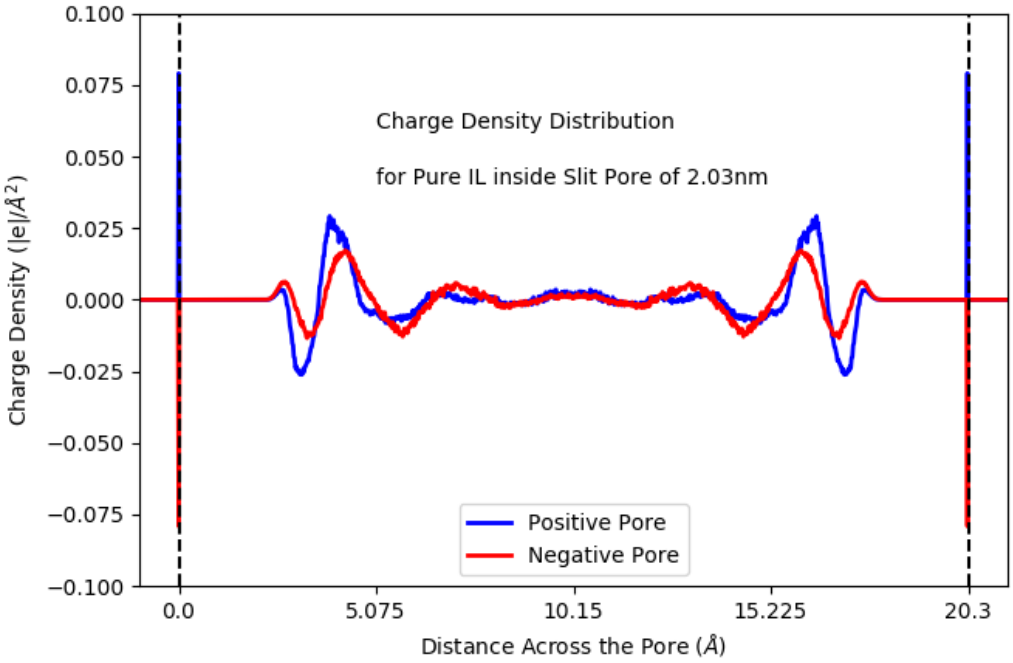

FIG. 2. Inside the $L = 2.03nm$ slit pore, charge density distribution comparison between positive and negative pores for pure ionic liquids.

C. Comparison between Total and Solvent Components

Figure 3 compares total and solvent charge densities (left) and electrostatic potential (right) at the largest slit pore with a size of $L = 2.03nm$. ACN solvent has a larger dipole moment of $3.9D$, while DCE has a dipole moment of $1.8D$. IL+ACN mixture reports a slightly higher capacitance than IL+DCE at this pore size. Charge profiles of ACN solvent closely resemble the total around the middle of the slit, while that of the DCE solvent remains relatively flat around the middle. For potential profiles, solvents component displays a smaller deviation from zero than total potential, as solvent molecule is neutral in charge on the whole.

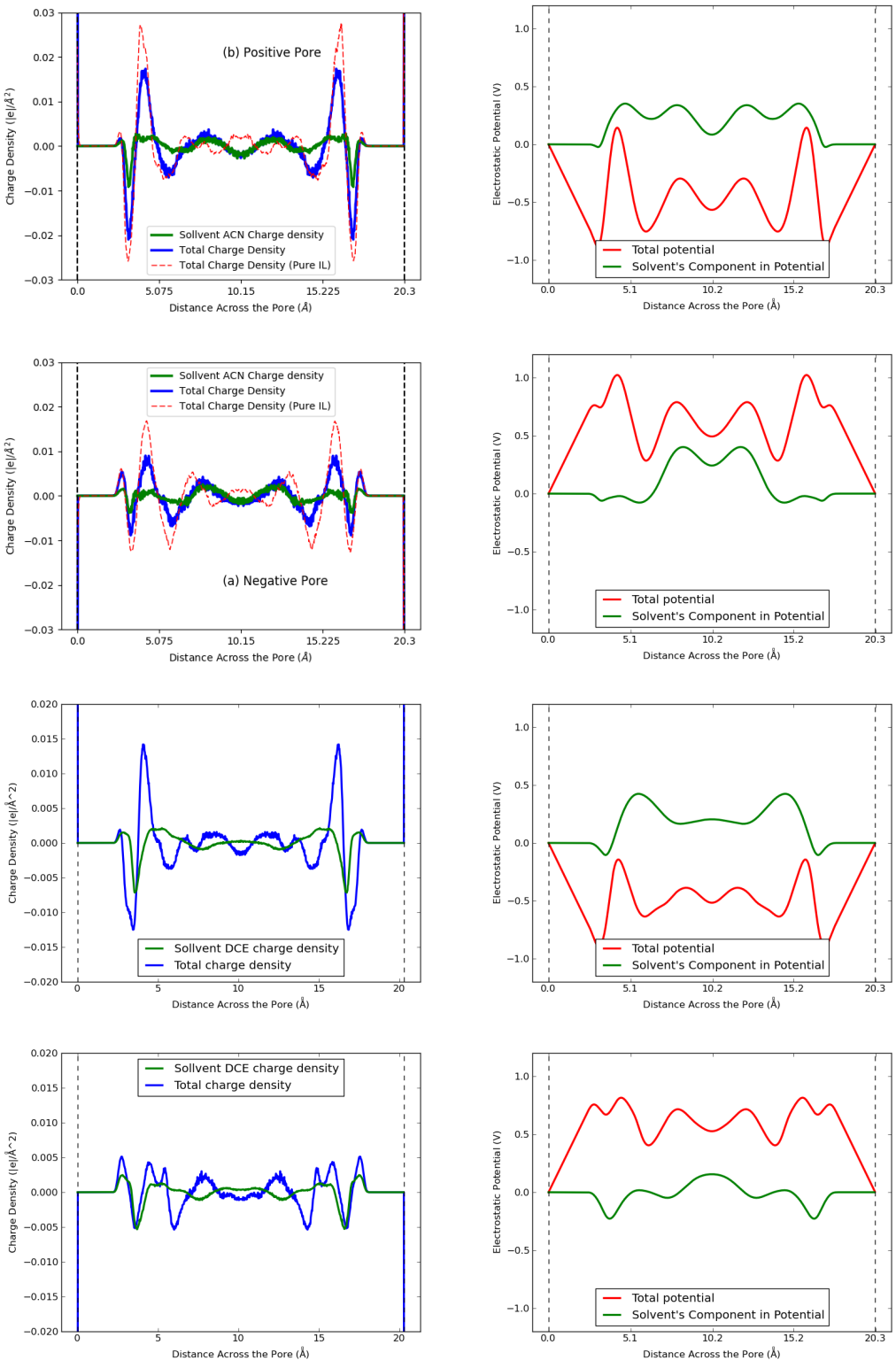

FIG. 3. Comparison between total and solvent charge densities (left) and electrostatic potential (right) for IL+ACN and IL+DCE mixtures inside positive and negative slit pores of $L = 2.03nm$ respectively.

III. NUMBER DENSITY IN SIDE VIEW

Complementary to the positive pore in the main text, Figure 4 displays the side view of number density distributions of IL mixtures inside negative slit pore.

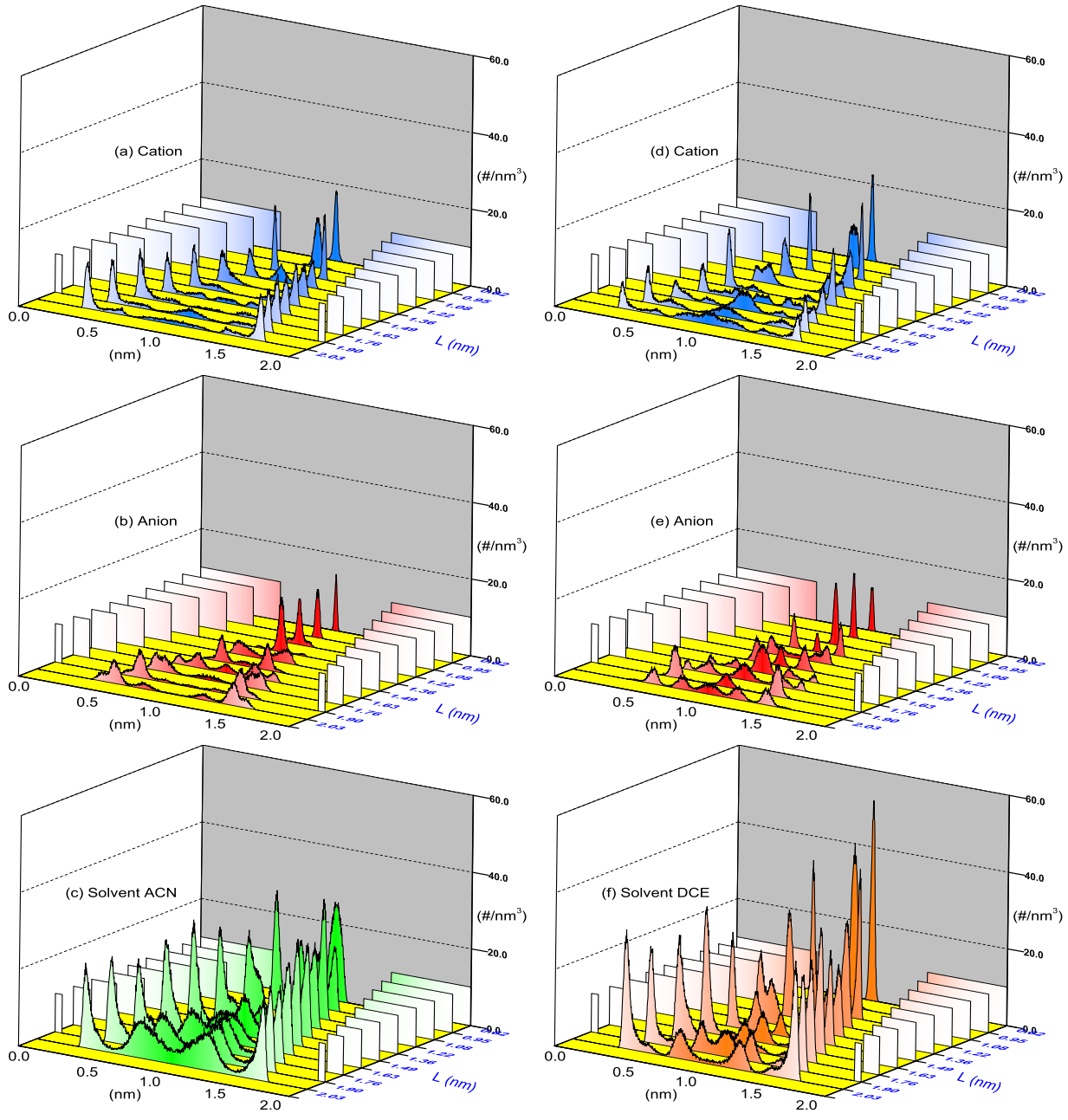

FIG. 4. Across the positive slit pore, number density distribution of (a) cations, (b) anions, (c) ACN solvent for IL+ACN mixture; and (d) cations (e) anions (f) DCE solvent for IL+DCE mixture, at a range of pore sizes and the charge density on electrode is $-0.253 C/m^2$.